Current Topics in Electrochemistry
Vol. 23, 2021

Original Article

The electrochemical performance of activated carbon nanofibers as a carbon electrode for supercapacitor applications: Effect of different electrolyte solutions

Erman Taer[1,*], Agustino[1], Awitdrus[1], Apriwandi[1], Amun Amri[2], Rika Taslim[3] and Zulkifli[1]

[1]Department of Physics, University of Riau, 28293 Simpang Baru, Pekanbaru, Riau;
[2]Department of Chemical Engineering, University of Riau, 28293 Simpang Baru, Pekanbaru, Riau;
[3]Department of Industrial Engineering, State Islamic University of Sultan Syarif Kasim, 28293 Simpang Baru, Riau, Indonesia.

ABSTRACT

Carbon materials with various structures have been investigated for use as electrode materials in supercapacitor devices. Therefore, this study aims to investigate the electrochemical performance of activated carbon nanofibers (ACNF) as a carbon electrode for supercapacitor applications in different aqueous electrolytes. Acidic (1M H_2SO_4), neutral (1M Na_2SO_4), and alkaline (1M KOH) electrolytes were used to investigate the electrochemical performance of the ACNF electrode. The morphology and elemental composition of the ACNF were studied using a scanning electron microscope (SEM) and energy dispersive X-ray spectroscopy (EDS). Furthermore, the Brunauer Emmet Teller (BET) and X-ray diffraction (XRD) were used to investigate the texture and structure of ACNF. The ACNF has fibers of diameter ranging from 45 nm to 56 nm. The ACNF has a high specific capacitance as well as a high energy density. Hence, the optimized aqueous electrolyte for the ACNF-based carbon electrode in the supercapacitor was determined to be in 1M H_2SO_4, with a specific capacitance of 214 F g^{-1} when compared to commonly used neutral (1M Na_2SO_4) and alkaline (1M KOH) electrolytes. This discovery is expected to boost the development of electrode materials for supercapacitor devices.

*Corresponding author: erman.taer@lecturer.unri.ac.id

KEYWORDS: electrochemical performance, activated carbon nanofibers, carbon electrode, aqueous electrolytes, supercapacitor.

1. INTRODUCTION

There has been continuous depletion of natural energy resources, drastic climate change, environmental concern, and rising energy consumption. Furthermore, over the last few decades, the research community has been challenged to discover and develop clean, green, renewable, environmentally friendly, and promising energy storage devices. The development of these devices is shifting toward renewable energy sources such as solar, hydro, and wind [1-5]. However, these resources make it difficult to meet the ever-increasing demand for energy in this decade. Due to their high power density [6, 7], fast charge/ discharge rate [7, 8], long life cycle [9-11] and rapid charge propagation dynamics [12, 13], supercapacitor (SC) is one of the most promising alternative energy storage devices. The electrolyte and electrode materials have a strong influence on the specific capacitance of SCs. Due to an electric double layer formed at the electrode/electrolyte interface, electrolyte compatibility with the electrode material is also important in the development [14]. In terms of cost, lifetime, low internal resistance, non-flammability, and toxicity, aqueous electrolytes are preferable to organic types for SC applications.

This is because the ion size compatibility with pore size, charge transfer resistance, and electrolyte ionic mobility is the major driving parameter for improved performance. Therefore, an understanding of electrode-electrolyte interaction is critical.

The other determining factor for supercapacitor electrochemical performance is the electrolyte [15]. Although solid/quasi-solid electrolytes can effectively prevent liquid electrolyte leakage during service, their application has been limited due to their low ionic conductivity, which limits the quick charging/discharging ability of supercapacitors [16]. Organic electrolytes, including ionic liquids, can work at higher voltages in liquids despite having low ionic conductivity and a high cost. Also, aqueous electrolytes are preferable to organic for SC applications in terms of cost, lifetime, low internal resistance, non-flammability, and toxicity. Furthermore, they can provide high capacitance and conductivity with a higher magnitude of ionic conductivity than organic electrolytes. Despite a limited potential window, they have been widely used in supercapacitor research and development [17].

Carbon materials with different structure like activated carbon (AC) [18-21], carbon nanofibers (CNFs) [22-25], carbon nanotubes (CNT) [26, 27], graphene [28, 29], and others have been studied as SC electrode materials. Carbon nanofibers have piqued the interest of researchers due to their unique chemical and physical properties, thermal stability, and ultra-high specific surface area, depending on their size and shape. The CNFs typically have diameters ranging from 10 to 500 nm and lengths ranging from 0.5 to 200 m. Also, increasing the surface area of carbon nanofibers is a critical approach to improving electrode performance. In this context, two main methods were used, namely (i) thermal etching with a chemical reagent or a gaseous atmosphere and (ii) blending with various polymers precursor.

In this study, the synthesis of activated carbon nanofibers (ACNF) made from a combination of fibrous and non-fibrous components of pineapple leaf, as well as their applications as electrode materials for SC devices is described. In general, polymer precursors such as polyacrylonitrile (PAN) [25, 30], polyimide [30], polymethyl methacrylate (PMMA) [31], polyvinylalcohol (PVA) [32, 33], polyvinylidene fluoride (PVDF)/Polyacrylonitrile (PAN) [34] etc. are used to synthesize carbon nanofibers. The synthesis of activated CNFs without the use of these materials was investigated. Many studies on the synthesis of carbon nanofibers from biomass have been published. For example, Taer *et al.* (2018) successfully synthesized CNFs from water chesnut and achieved specific capacitance of 130 F g^{-1} [35]. Meanwhile, Taer *et al*. (2020) obtained the specific capacitance of 113 F g^{-1} for the carbon nanofiber made from Acacia leaf [36]. In addition, Taer *et al*. (2021) reported a simple method for the synthesis of carbon nanofibers derived from pineapple leaf fibers and obtained a specific capacitance of 191 F g^{-1} with a surface area of 945 m^2 g^{-1} [37]. Therefore, this study aims to investigate the effects of various aqueous electrolytes on the SC electrode performance. The electrochemical performance of the ACNF is presented. ACNFs have a high specific surface area of 1078 m^2 g^{-1} and a high optimum specific capacitance of 214 F g^{-1}.

2. EXPERIMENTS AND METHODS

2.1. Sample preparation

The fibrous and non-fibrous components of pineapple leaf were used as raw materials. The processing of raw materials was according to previously reported work [37]. Potassium hydroxide was used as a chemical reagent to produce activated carbon nanofibers. The carbonization was conducted using N_2 at a temperature of 600 °C followed by CO_2 activation at 850 °C for 2.5 h with a heating rate of 10 °C min^{-1}; this process was according to previously reported work [37-39]. Finally, to remove the activating agent and impurities, the activated carbon was washed using distilled water until pH is neutral and dried at 110 °C for 48 h.

2.2. Material characterization

SEM and EDS were used to examine the morphology and elemental compositions of activated carbon nanofibers (JEOL-JSM 6510LA). The X-ray diffraction pattern was observed using an X-ray diffractometer (XRD, Shimadzu 7000) with a CuKα light source at 0.154 nm. Furthermore, the textural structures of activated carbon nanofibers (ACNF) were studied using nitrogen gas adsorption/ desorption and measured at -196 °C with a

Quantachrome TouchWin V.1.2 instrument. The BET and BJH methods were used to calculate and evaluate the sample's specific surface area and pore size distributions.

2.3. Electrochemical characterization

Cyclic voltammetry (CV) and galvanostatic charge-discharge (GCD) methods were used to examine the electrochemical performance of the electrode. The CV and GCD measurements were performed in different electrolyte solution i.e. acidic (1M H_2SO_4), neutral (1M Na_2SO_4), and alkaline (1M KOH) electrolytes using a two-electrode configuration. During the measurement, the voltage window range was set at 0-1 V and at scan rates of 1 mV s^{-1}. The specific capacitance of the ACNF was calculated by the equation:

$$C_{sp} = \frac{2Ix\Delta t}{\Delta Vxm} \quad (1)$$

where I = discharge current, Δt = discharge time, ΔV = voltage, and m = electrode mass. The energy density (E) and power density (P) were obtained following the equations:

$$E = \frac{1}{2}CV^2 / 3.6 \quad (2)$$

$$P = \frac{E}{\Delta t}x3600 \quad (3)$$

where E = energy density, P = power density, C = specific capacitance, V = voltage, Δt = discharge time.

3. RESULTS AND DISCUSSION

3.1. Physical property analysis

Figure 1 shows the SEM image and EDS spectrum of the ACNF sample. The surface morphology of the ACNF is displayed in Figure 1a. Morphologically, the fibers appeared uniform and were interconnected with one another. Ion transfer within the carbon matrix was facilitated by the form of an interconnected porous structure. The inter-fiber connection affected the electrode performance in carbon electrodes with nanofiber structures. This was due to the inter-fiber connection that shortens the charge transport route within the carbon electrode network, improves charge transfer efficiency, and lowers the internal resistance [25]. The fibers had a diameter in the range of 45-156 nm. Figure 1b displays the EDS spectrum of the ACNF sample. The elemental composition of the ACNF sample includes carbon (91.26 %), oxygen (5.79 %), magnesium (1.62 %), potassium (0.53 %), and calcium (0.83 %).

The XRD patterns of the ACNF (Figure 2) showed two wide peaks at angles of 23° and 43°, corresponding to the 002 and 100 planes. The 002 plane reflected the graphite structure of the ACNF [40], whereas the 100 plane indicates an amorphous structure of the electrode [41-43]. The interlayer distance (d_{002}) and graphite crystalline thickness (L_{002}) based on XRD data were calculated, being 0.372 nm and 0.49 nm, respectively.

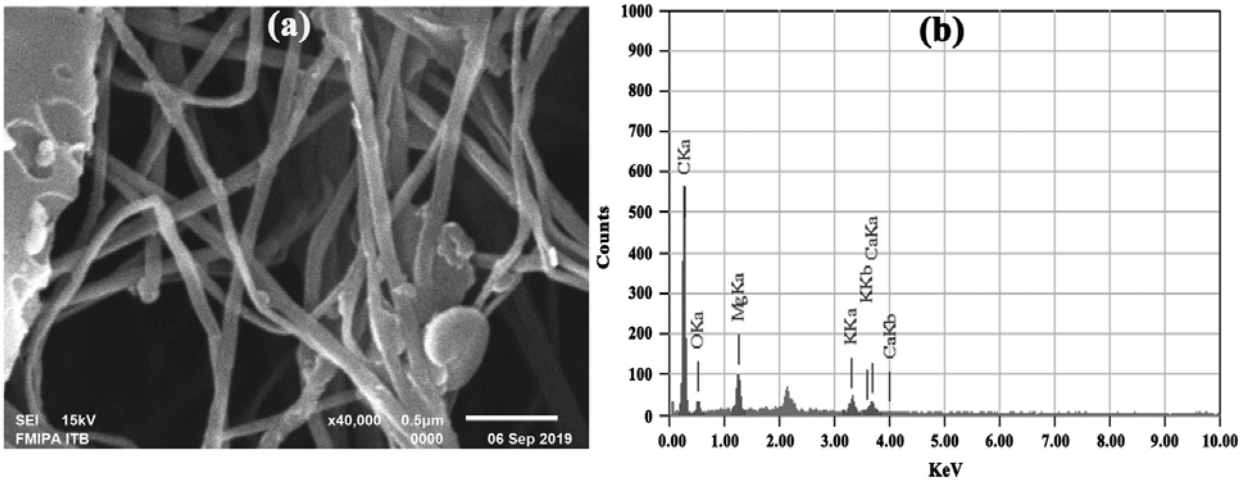

Figure 1. (a) SEM micrograph and **(b)** EDS spectrum of the ACNF sample.

Figure 3 shows the adsorption-desorption of N_2 gas at -196 °C, as well as the pore size distributions. As seen, the ACNF sample (Figure 3a) exhibited a type IV isotherm, indicating that it contains mesoporous materials. This was due to a hysteresis loop caused by capillary condensation in the mesopores. The existence of hysteresis loops at relative pressures (P/P_0) ranging from 0.45 to 0.9 atm revealed the presence of mesopores [44, 45]. Furthermore, small tails were found in the ACNF isotherms at relative pressures close to 1.0 atm, indicating the presence of macropores in the ACNF sample [28, 46]. The specific surface area of the ACNF sample was 1078 m^2 g^{-1}, which was much higher than that of PALF electrode as per a previous report (945 m^2 g^{-1}). The physical and chemical properties of the precursor and the processing parameters including activated conditions such as activation temperature [47, 48], activating agent [48, 49], and molarities of activating agent can result in increased surface area. Also, volume total and average pore radius of the ACNF sample (Figure 3b) were 0.579 cm^3 g^{-1} and 1,075 nm, respectively. With the average pore radius of 1.075 nm, ion migration and diffusion can be facilitated, thereby improving the electrochemical performance of the ACNF sample [50].

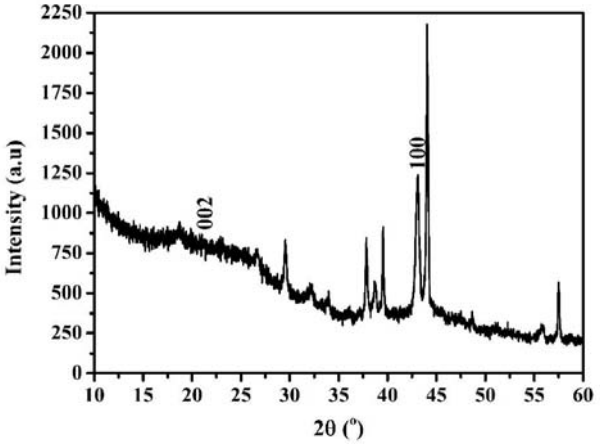

Figure 2. XRD pattern of the ACNF sample.

3.2 Electrochemical performance

Cyclic voltammetry (CV) and GCD measurements were carried out in different aqueous electrolytes, namely 1M H_2SO_4, 1M Na_2SO_4, and 1M KOH. Based on the aqueous electrolyte, the ACNF electrode was denoted as ACNF-1, ACNF-2, and ACNF-3, respectively. During the CV and GCD measurement, the ACNF sample was polished into 8 mm in diameter and 0.2 mm in thickness. The ACNF sample was formed into electrodes and their electrochemical performance in symmetrical cells was evaluated. Figure 4 shows a comparison of the CV curves of ACNF-1, ACNF-2, and ACNF-3 at a scan rate of 1 mV s^{-1}. Therefore, all of the ACNF electrode CV curves were ideally rectangular-shaped curves without any visible redox peaks. Based on this test, it was predicted that ACNF-1 would have the best electrochemical performance of the three aqueous electrolytes.

Figure 5a shows the GCD curves for ACNF-1, ACNF-2, and ACNF-3. The electric double layer

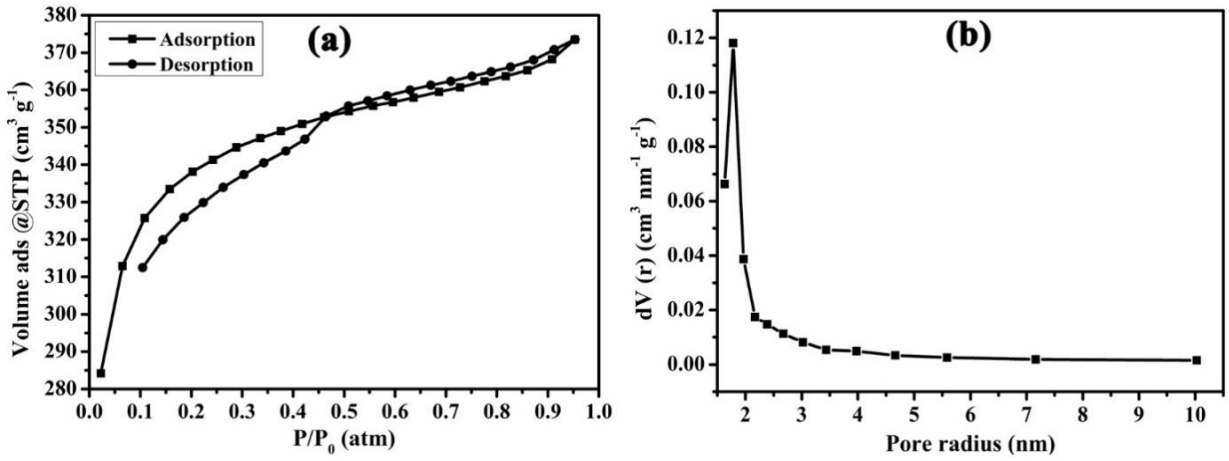

Figure 3. (a) N_2 adsorption/desorption and **(b)** pore size distributions of the ACNF sample.

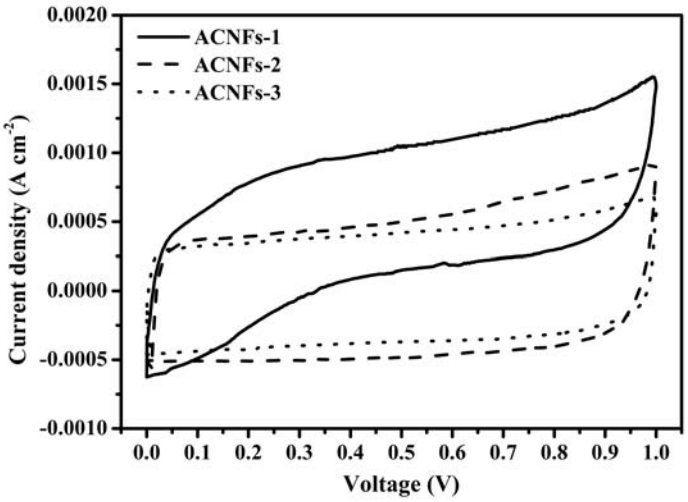

Figure 4. Cyclic voltammogram of the ACNF samples.

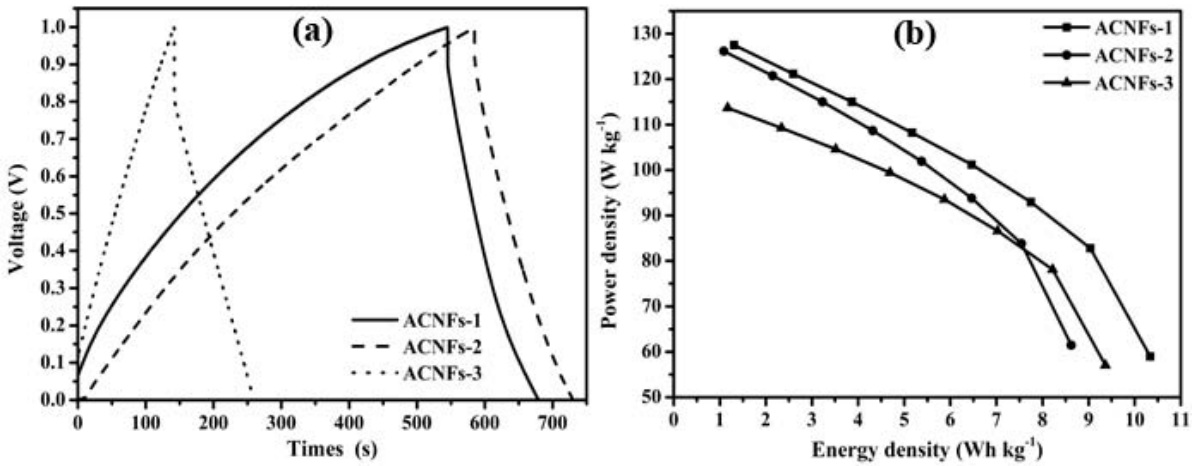

Figure 5. Galvanostatic charge/discharge (**a**) and Ragone plot (**b**) of the ACNF samples.

charge/discharge mechanism was confirmed by the linear and symmetrical charge/discharge characteristics of ACNF-1, ACNF-2, and ACNF-3. Also, the galvanostatic charge-discharge profile did not show any pseudocapacitance. ACNF-1, ACNF-2, and ACNF-3 had IR drop values of 0.039 mΩ, 0.062 mΩ, and 0.071 mΩ, respectively. According to the CV data, the specific capacitance of ACNF was 214 F g^{-1} for ACNF-1, 196 F g^{-1} for ACNF-2, and 173 F g^{-1} for ACNF-3. Figure 5b shows the energy density as a function power density of the ACNF displayed in Ragone plots based on GCD curves. It can then be seen that the ACNF-1 can reach a maximum energy density of 10.34 Wh kg^{-1}, which was higher than the 8.62 Wh kg^{-1} of ACNF-2 and 9.37 Wh kg^{-1} of ACNF-3. All the electrochemical performance of ACNF demonstrated that ACNF material produces an excellent electrode that works well in different aqueous electrolytes. The better electrochemical performance of ACNF in 1M H_2SO_4 than in 1M Na_2SO_4 and 1M KOH may indicate a good ion diffusion in the electrode layer of H^+ and SO_4^{2-} ions during the charge/discharge process. Furthermore, differences in electrochemical performance in different electrolytes can be attributed to ion permeability into the active matrix [51]. Accessibility into the matrix varied with hydrated radius, ionic

Table 1. The specific capacitances (C_{sp}) of the ACNF compared to previously reported activated carbon nanofibers.

Materials	Electrolyte	Electrochemical test	C_{sp} (F g^{-1})	References
Mesoporous ribbon-shaped graphitic carbon nanofibers	6M KOH	GCD	228	[22]
Polyacrylonitrile (PAN) and novolac (NOC)	2M KOH	GCD	394	[25]
Nanostructural carbon nanofibers	2M KOH	GCD	210	[31]
Water chesnut	1M H_2SO_4	CV	130	[35]
Acacia leaf	1M H_2SO_4	CV	113	[36]
Pineapple leaf fibers	1M H_2SO_4	CV	191	[37]
PAN fibers	Ionic liquid	GCD	148	[57]
Fibrous and non-fibrous components of pineapple leaf	1M H_2SO_4 1M Na_2SO_4 1M KOH	GCD	214 196 173	This work

mobility, and molar ionic conductivity [52]. The hydrated radius of H^+, K^+, and Na^+ in the electrolytes H_2SO_4, KOH, and Na_2SO_4 were 0.28 nm, 0.331 nm, and 35.8 nm, respectively [53, 54]. Furthermore, the ionic conductivities of H+ in H_2SO_4, K^+ in KOH, and Na^+ in Na_2SO_4 were 350.1 S cm^2 mol^{-1}, 73.5 S cm^2 mol^{-1}, and 50.11 S cm^2 mol^{-1}, respectively [55, 56]. The H_2SO_4 electrolyte solution produced the highest specific capacitance of the ACNF due to its lower cationic radius, higher ionic mobility, and higher ionic conductivity. The optimum specific capacitance obtained from ACNF-2 was 214 F g^{-1} at current 1.0 A. These specific capacitances of the ACNF are well within the range of previously reported activated carbon nanofibers, which are listed in Table 1.

4. CONCLUSION

In summary, aqueous electrolytes with different properties, i.e, acidic (1M H_2SO_4), neutral (1M Na_2SO_4), and alkaline (1M KOH) were used to investigate the electrochemical performance of the ACNF-based carbon electrode in supercapacitor devices. According to SEM micrographs, the ACNF has fibers of diameter ranging from 45 to 156 nm. Furthermore, the 1M H_2SO_4 electrolyte was found to have better electrochemical performance for the ACNF-based carbon electrode, with a higher specific capacitance of 214 F g^{-1} compared to the neutral and alkaline electrolytes. In addition, the practical effect of an acidic electrolyte (1M H_2SO_4) on the ACNF-based carbon electrode demonstrated a high specific capacitance and energy density.

ACKNOWLEDGEMENTS

The authors are grateful for financial support from Kementerian Pendidikan, Kebudayaan, Riset, dan Teknologi Republik Indonesia through the third year basic research grant 2021 (contract no. 1418/UN.19.5.1.3/PT.01.03/2021).

CONFLICT OF INTEREST STATEMENT

There are no conflicts of interest.

REFERENCES

1. Chen, X., Li, C., Grätzel, M., Kostecki, R. and Mao, S. S. 2012, Chem. Soc. Rev., 41, 7909.
2. Yan, J., Wang, Q., Wei, T. and Fan, Z. 2014, Adv. Energy Mater., 4, 1308816.
3. Liu, Y., Huang, B., Lin, X. and Xie, Z. 2017, J. Mater. Chem. A., 5, 25090.
4. Bi, Z., Kong, Q., Cao, Y., Sun, G., Su, F., Wei, X., Li, X., Ahmad, A., Xie, L. and Chen, C. M. 2019, J. Mater. Chem. A., 7, 16028.
5. Wang, Y., Qu, Q., Gao, S., Tang, G., Liu, K., He, S. and Huang, C. 2019, Carbon N. Y., 155, 706.

6. Jayalakshmi, M. and Balasubramanian, K. 2008, Int. J. Electrochem. Sci., 3, 1196.
7. Bose, S., Kuila, T., Mishra, A. K., Rajasekar, R., Kim, N. H. and Lee, J. H. 2012, J. Mater. Chem., 22, 767.
8. Winter, M. and Brodd, R. J. 2004, Chem. Rev., 104, 4245.
9. Kim, B. K., Sy, S., Yu, A. and Zhang, J. 2015, Handb. Clean Energy Syst., 1
10. Heimböckel, R., Kraas, S., Hoffmann, F. and Fröba, M. 2018, Appl. Surf. Sci., 427, 1055.
11. Guo, F., Jiang, X., Jia, X., Liang, S., Qian, L. and Rao, Z. 2019, J. Electroanal. Chem., 844, 105.
12. Suárez, L. and Centeno, T. A. 2020, J. Power Sources, 448, 227413.
13. Vinayagam, M., Babu, R. S., Sivasamy, A. and Ferreira de Barros, A. L. 2020, Biomass and Bioenergy., 143, 105838.
14. Daraghmeh, A., Hussain, S., Saadeddin, I., Servera, L., Xuriguera, E., Cornet, A. and Cirera, A. 2017, Nanoscale Res. Lett., 12, 639.
15. Cheng, M., Meng, Y. N. and Wei, Z. X. 2018, Isr. J. Chem., 58, 1299.
16. Choudhury, N. A., Sampath, S. and Shukla, A. K. 2009, Energy Environ. Sci., 2, 55.
17. Zhang, Y., Yu, S., Lou, G., Shen, Y., Chen, H., Shen, Z., Zhao, S., Zhang, J., Chai, S. and Zou, Q. 2017, J. Mater. Sci., 52, 11201.
18. Taer, E., Mardiah, M. A., Agustino, A., Mustika, W. S., Apriwandi, A. and Taslim, R. 2021, J. Appl. Eng. Sci., 19, 162.
19. Ma, F., Ding, S., Ren, H. and Liu, Y. 2019, RSC Adv., 9, 2474.
20. Elaiyappillai, E., Srinivasan, R., Johnbosco, Y., Devakumar, P., Murugesan, K., Kesavan, K. and Johnson, P. M. 2019, Appl. Surf. Sci., 486, 527.
21. Sesuk, T., Tammawat, P., Jivaganont, P., Somton, K., Limthongkul, P. and Kobsiriphat, W. 2019, J. Energy Storage., 25, 100910.
22. Ma, C., Cao, E., Li, J., Fan, Q., Wu, L., Song, Y. and Shi, J. 2018, Electrochim. Acta., 292, 364.
23. Xu, J., Zhang, L., Xu, G., Sun, Z., Zhang, C., Ma, X., Qi, C., Zhang, L. and Jia, D. 2018, Appl. Surf. Sci., 434, 112.
24. Yanilmaz, M., Dirican, M., Asiri, A. M. and Zhang, X. 2019, J. Energy Storage., 24, 100766.
25. Wang, H., Niu, H., Wang, H., Wang, W., Jin, X., Wang, H., Zhou, H. and Lin, T. 2021, J. Power Sources., 482, 228986.
26. Gao, Z., Song, N., Zhang, Y., Schwab, Y., He, J. and Li, X. 2018, ACS Sustain. Chem. Eng., 6, 11386.
27. Wu, C., Zhang, S., Wu, W., Xi, Z., Zhou, C., Wang, X., Deng, Y., Bai, Y., Liu, G., Zhang, X., Li, X., Luo, Y. and Chen, D. 2019, Carbon N. Y., 150, 311.
28. Fan, Y. M., Song, W. L., Li, X. and Fan, L. Z. 2017, Carbon N. Y., 111, 658.
29. Niu, Q., Gao, K., Tang, Q., Wang, L., Han, L., Fang, H., Zhang, Y., Wang, S. and Wang, L. 2017, Carbon N. Y., 123, 290.
30. Bui, H. T., Kim, D. Y., Kim, D. W., Suk, J. and Kang, Y. 2018, Carbon N. Y., 130, 94.
31. Lai, C. C. and Lo, C. T. 2015, Electrochim. Acta., 183, 85.
32. Kebabsa, L., Kim, J., Lee, D. and Lee, B. 2020, Appl. Surf. Sci., 511, 145313.
33. Widiyastuti, W., Rois, M. F., Suari, N. M. I. P. and Setyawan, H. 2020, Adv. Powder Technol., 31, 3267.
34. Heo, Y. J., Zhang, Y., Rhee, K. Y. and Park, S. J. 2019, Compos. Part B Eng., 156, 95.
35. Taer, E., Zulkifli., Awitdrus., Taslim, R., Agustino, A. and Apriwandi. 2018, Curr. Top. Electrochem., 20, 39.
36. Taer, E., Natalia, K., Apriwandi, A., Taslim, R., Agustino, A. and Farma, R. 2020, Adv. Nat. Sci. Nanosci. Nanotechnol., 11, 25007.
37. Taer, E., Agustino, A., Awitdrus, A., Farma, R. and Taslim, R. 2021, J. Electrochem. Energy Convers. Storage., 18, 031004.
38. Agustino., Awitdrus., Amri, A., Taslim, R. and Taer, E. 2020, J. Phys. Conf. Ser., 1655, 012008.
39. Taer, E., Apriwandi, A., Krisman., Minarni., Taslim, R., Agustino, A. and Afrianda, A. 2018, J. Phys. Conf. Ser., 1120, 012006.
40. Sodtipinta, J., Ieosakulrat, C., Poonyayant, N., Kidkhunthod, P., Chanlek, N., Amornsakchai, T. and Pakawatpanurut, P. 2017, Ind. Crops Prod., 104, 13.
41. Bonino, F., Brutti, S., Reale, P., Scrosati, B., Gherghel, L., Wu, J. and Müllen, K. 2005, Adv. Mater., 17, 743.
42. Zhang, L. L. and Zhao, X. S. 2009, Chem. Soc. Rev., 38, 2520.

43. Senthilkumar, S. T., Senthilkumar, B., Balaji, S., Sanjeeviraja, C. and Selvan, R. K. 2011, Mater. Res. Bull., 46, 413.
44. Peng, C., Yan, X. B., Wang, R. T., Lang, J. W., Ou, Y. J. and Xue, Q. J. 2013, Electrochim. Acta., 87, 401.
45. Ouyanga, T., Chenga, K., Yang, F., Zhou, L., Zhu, K., Ye, K., Wang, G. and Cao, D. 2017, J. Mater. Chem. A., 5, 14551.
46. Nagaraju, G., Cha, S. M. and Yu, J. S. 2017, Sci. Rep., 7, 45201.
47. Zhao, X., Cao, J., Morishita, K., Ozaki, J. and Takarada, T. 2010, Energy and Fuels, 24, 1889.
48. Roldan, S., Villar, I., Rui, V., Blanco, C., Granda, M., Menendez, R. and Santamarıa, R. 2010, Energy fuelsels., 24, 3422.
49. Subramanian, V., Luo, C., Stephan, A. M., Nahm, K. S. and Thomas, S. 2007, J. Phys. Chem. C, 111, 7527.
50. Li, Y., Ou-Yang, W., Xu, X., Wang, M., Hou, S., Lu, T., Yao, Y. and Pan, L. 2018, Electrochim. Acta., 271, 591.
51. Ruiz, V., Santamaría, R., Granda, M. and Blanco, C. 2009, Electrochim. Acta., 54, 4481.
52. Zhu, J., Xu, Y., Wang, J., Lin, J., Sun, X. and Mao, S. 2015, Phys. Chem. Chem. Phys., 17, 28666.
53. Nightingale, E. R. 1959, J. Phys. Chem., 63, 1381.
54. Kiriukhin, M. Y. and Collins, K. D. 2002, Biophys. Chem., 99, 155
55. Burke, A. 2007, Electrochim. Acta., 53, 1083.
56. Yu, A., Chabot, V. and Zhang, J. 2017, Electrochemical supercapacitors for energy storage and delivery: Fundamentals and applications, CRC Press, Taylor & Francis Group.
57. He, T., Fu, Y., Meng, X., Yu, X. and Wang, X. 2018, Electrochim. Acta., 282, 97.